Desalination and Water Treatment
www.deswater.com
doi: 10.1080/19443994.2013.801792

52 (2014) 4369–4375
June

Taylor & Francis
Taylor & Francis Group

Fluoride removal from aqueous solution by functionalized-polyacrylonitrile coated with iron oxide nano particles: characterization and sorption studies

Jafar Nouri[a], Ramin Nabizadeh[b], Mahsa Jahangiri-rad[a,*], Masoud Yunesian[b] Faramarz Moattar[a]

[a]*Department of Environmental Science, Graduate School of the Environment and Energy, Science and Research Branch, Islamic Azad University, Tehran, Iran*
Tel. +98 21 4486 9443; email: mahsajahangiri_64@yahoo.com
[b]*Center for Air Pollution Research, Institute of Environmental Research, Tehran University of Medical Sciences, Tehran, Iran*

Received 21 January 2013; Accepted 27 April 2013

ABSTRACT

Polyacrylonitrile (PAN)-oxime-nano Fe_2O_3 was used as an adsorbent for the removal of fluoride from water. The influences of contact time, initial fluoride concentration, and adsorbent dosage were investigated by batch equilibrium studies. The rate of adsorption was rapid with equilibrium being attained after 100 min. The Langmuir isotherm model was found to represent the measured adsorption data well. The adsorption process followed the pseudo-first-order kinetic model. It was found that the adsorbed fluoride could be easily desorbed by replacing the adsorbent in deionized water. This indicates that the material could be easily recycled. The results from the present study show the potential of PAN-oxime-nano Fe_2O_3 for fluoride removal. Furthermore, the adsorption isotherms of Fluoride removal were examined and the possible desorption process was discussed.

Keywords: Polyacrylonitrile; Fe_2O_3 nanoparticles; Adsorption isotherms; Desorption

1. Introduction

Fluoride contamination in drinking water due to natural and anthropogenic activities has received great attention. Fluoride has both beneficial and detrimental effects on health. World Health Organization (WHO) has set the upper threshold of fluoride level as 1.5 mg/L [1]. Dental and skeletal fluorosis occurs due to excess uptake of fluoride through drinking water [2]. Lower levels of fluoride in drinking water may lead to dental caries [3]. Several methods have been applied to remove excessive fluoride from aqueous environments including, precipitation and coagulation processes [4], activated alumina [5], calcium [6], and alum sludge [7], ion exchange [8], electrodialysis [9], and electrochemical methods [10]. Among the various methods used for defluoridation, the adsorption process is widely used due to the simplicity of its design and operation and its low cost [11–13]. In the past few years, novel nano adsorbents with strong affinity towards fluoride removal have been applied such as

*Corresponding author.

1944-3994/1944-3986 © 2013 Balaban Desalination Publications. All rights reserved.

Fe_3O_4@Al $(OH)_3$ magnetic nanoparticles [14], nano hydroxyapatite/chitisan [15], and synthesized nanoparticles of MgO [16]. Polyacrylonitrile (PAN) and its copolymers have been widely studied for commercial/technological exploitations. Cross-linking of PAN will impart some of its important physical properties such as insolubility and resistance to swelling in common solvents [17,18].

The high crystalline melting point (317˚C) of PAN and its limited solubility in certain solvents is due to the intermolecular forces between the polymer chains [19]. Active nitrile groups present in PAN copolymers allow the introducing of new functional groups by special reaction. Researchers have reported various methods of PAN modification to obtain cationite, anionite, and ampholyte [20]. In the present study, PAN-oxime was synthesized through the modification of PAN and the modified PAN was coated with iron oxide nanoparticles (Fe_2O_3). The PAN-oxime-nano Fe_2O_3 was subsequently used for the adsorption of fluoride.

2. Experimental

2.1. Preparation of PAN-oxime-nano Fe_2O_3

Fig. 1 represents the reaction of hydroxilamine hydrochloride with PAN nitrile group. Hydroxilamine hydrochloride (16 g), sodium carbonate (12 g), and 0.4 g of PAN powder were added to a 250 ml bottle to which 100 ml of deionized water was added and shaken. The reaction was carried out at 70˚C for 120 min. After reaction, the resultant was filtered and let to dry. Fe_2O_3 was coated on PAN functionalized by adding 0.2 g of selected Fe_2O_3 and 100 ml deionized water in a sealed bottle. The solution was shaken at 70˚C for 120 min. The resultant was filtered and dried in a vacuum oven at 60˚C. PAN functionalized-Fe_2O_3 was used as an adsorbent.

2.2. Characterization of the adsorbent

The functional group and iron oxide nanoparticles on PAN were detected by Fourier transform infrared (FT-IR) spectrometer. The size and structure of the synthesized functionalized-PAN coated with Fe_2O_3 nanoparticles were analyzed by transmission electron microscopy (TEM). X-ray diffraction (XRD) measurements of the catalyst powder were recorded using a Philips PW 1800 diffractometer. The FT-IR spectra of the samples were recorded on the FT-IR Brucker Tensor 27 spectrometer. The particle size and morphology of the nanocrystalline particle were examined using transmission electron microscope TEM (LEO 912AB).

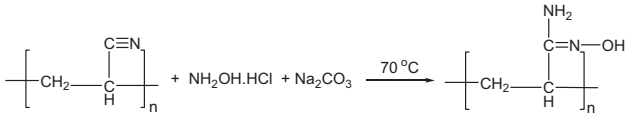

Fig. 1. Functionalization of PAN with hydroxylamine hydrochloride.

2.3. Batch adsorption experiments

A stock solution (1,000 mg/L) was prepared by dissolving sodium fluoride in 1 L of deionized water. This was diluted to obtain the required concentrations for further use. All batch adsorption experiments were carried out in 50 ml sealed plastic tubes with the working volume of 25 ml. After adding a known weight of the adsorbent, the flask was shaken (150 rpm) for 24 h on a horizontal rotary shaker. The liquid samples were then centrifuged and the residual fluoride was analyzed by use of fluoride-specific ion indicating electrode. The amount of fluoride adsorbed was calculated from the following equation:

$$q_e = (C_0 - C_e)V/m \quad (1)$$

where q_e is the fluoride adsorbed (mg/g), C_0 and C_e are the initial and equilibrium concentrations of fluoride in solution (mg/L), respectively; V is the volume of solution (L), and m is mass of the adsorbent (g).

2.4. Desorption studies

Desorption studies were initiated by replacing half of the adsorption equilibrium supernatant solution after centrifugation with the corresponding fluoride-free background electrolyte solution to the equal volume. Desorption experiments were carried out in the dark at 25 ± 2˚C for 24 h each time as conducted for adsorption experiments, and performed three times sequentially in order to examine the stability of the adsorption and the hysteresis of the desorption of the fluoride.

3. Results

3.1. Adsorbent characteristics

Fig. 2 shows the FT-IR spectra of the PAN and functionalized PAN. The FT-IR spectrum of PAN (Fig. 2(a)) exhibited the characteristic bands of nitrile (2,238 cm^{-1}), carbonyl (1,728 cm^{-1}), and ether (1,229 and 1,070 cm^{-1}) groups; carbonyl and ether bands come from methylacrylate comonomer. The FT-IR

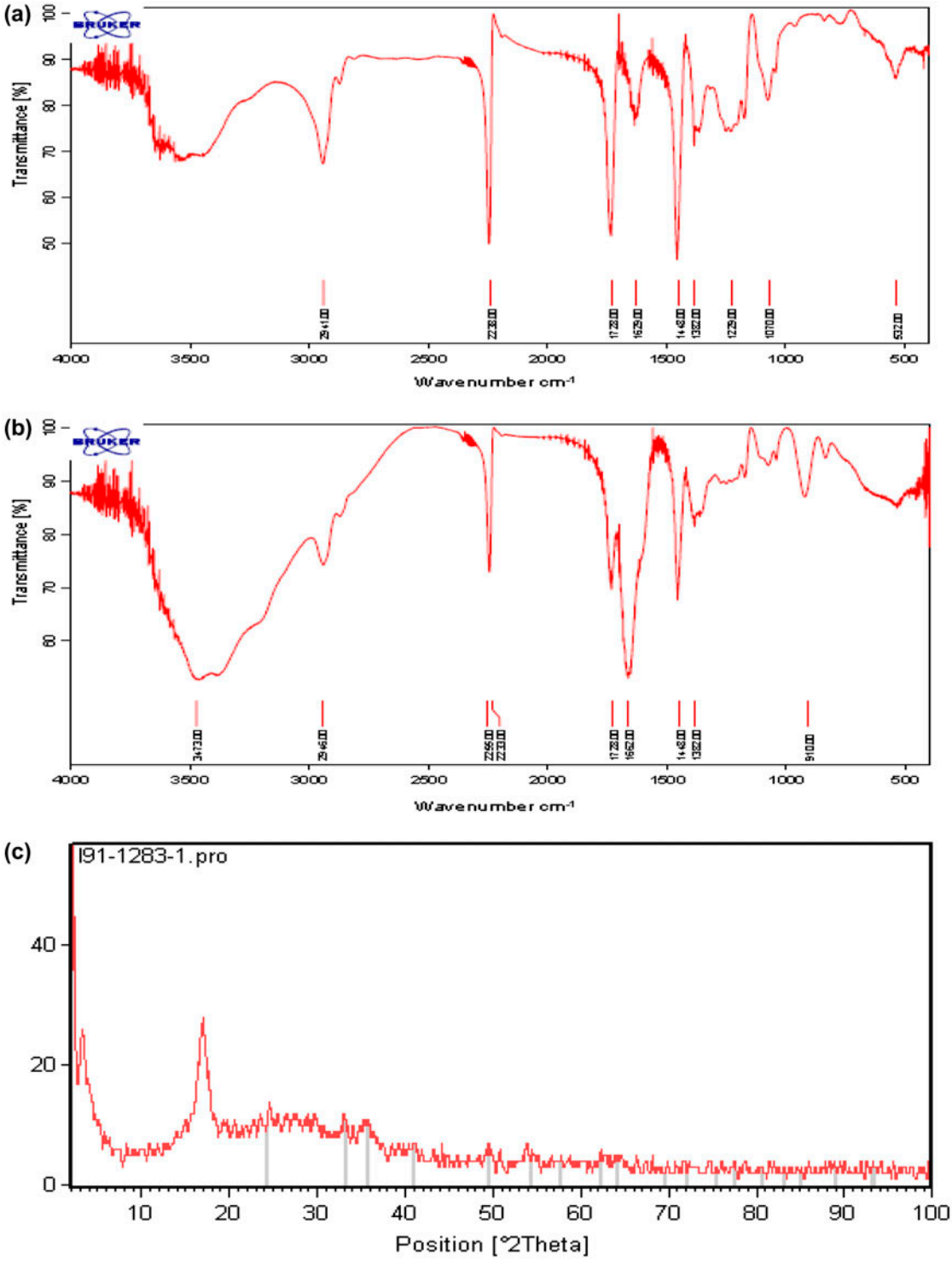

Fig. 2. FT-IR pattern of PAN (a), functionalized PAN (b), and XRD pattern of oxime-nano Fe_2O_3 (c).

spectra of functionalized PAN (Fig. 2(b)) showed all the characteristic bands of the functional groups of PAN with additional peaks at 910 and 1,662 cm^{-1}, which are due to the stretching vibration of N–O and C=N groups in functionalized PAN, respectively [21]. Furthermore, the intensity of the nitrile peak of functionalized PAN decreased; all of these changes confirm the introduction of amidoxime groups on

PAN. Fig. 2(c) shows the XRD patterns of Fe_2O_3 nanoparticles and functionalized-PAN—Fe_2O_3. The XRD patterns of functionalized-PAN—Fe_2O_3 (Fig. 2(c)) show a broad noncrystalline peak ($2\theta = 20^\circ$–30°) and a crystalline peak ($2\theta = 18^\circ$) corresponding to the orthorhombic PAN (110) reflection; and besides the diffraction peaks of the PAN phase, another peak appeared corresponding to the above peaks indicating that the Fe_2O_3 nanoparticles on the PAN have the same crystal diffraction as pure Fe_2O_3 [22]. The morphologies of the adsorbent are characterized by TEM (see Fig. 2). As shown in Fig. 3, Fe_2O_3 nanoparticles are attached to the surface of functionalized-PAN.

3.2. Sorption experiment/adsorption isotherm

The isotherm models of langmuir and freundlich were used to fit the experimental adsorption equilibrium data of fluoride on PAN-Oxime-nano Fe_2O_3. These two models are represented as follows:

$$\frac{1}{q_e} = \frac{1}{q_m} + \frac{1}{q_m b C_e} \text{ Langmuir isotherm} \quad (2)$$

$$q_e = K_f C_e^{1/n} \text{ Freundlich isotherm} \quad (3)$$

where C_e ($mg\,l^{-1}$) is the equilibrium concentration, q_e ($mg\,g^{-1}$) is the amount of adsorbate adsorbed per unit mass of adsorbate, and q_m and b are the Langmuir constants related to adsorption capacity and rate of adsorption, respectively. K_f and $1/n$ are the freundlich constants related to the adsorption capacity and intensity, respectively.

Application of Langmuir and Freundlich models to the adsorption isotherm showed that both models provided excellent satisfactory fitness with high R^2 values (0.956 and 0.989). The estimated values for the parameters of these models are shown in Table 1. In order to investigate the adsorption process of fluoride on PAN-oxime-nano Fe_2O_3, kinetic analysis was conducted using pseudo-first-order, pseudo-second-order, and intraparticle diffusion models. The Lagergren rate equation is one of the most widely used adsorption rate equations for the adsorption of solute from a liquid solution. The pseudo-first-order kinetic model of Lagergren may be represented as:

$$\ln(q_e - q_t) = \ln(q_e) - k_1 t \quad (4)$$

where q_e and q_t are the amounts of dye adsorbed (mg/g) at equilibrium at time t (min), respectively; and k_1 is the rate constant of pseudo-first-order adsorption (min^{-1}). The validity of the model can be checked by linearized plot of $\ln(q_e - q_t)$ vs. t. The rate constant of pseudo-first-order adsorption is determined from the slope of the plot. The pseudo-second-order equation based on adsorption equilibrium capacity can be expressed as [23]:

$$t/q = 1/k_2 q_e^2 + t/q_e \quad (5)$$

Since neither the pseudo-first-order nor the pseudo-second-order model can identify the diffusion mechanism, the kinetic results were analyzed by the intraparticle diffusion model to elucidate the diffusion mechanism. This model is expressed as [24]:

$$q_t = k_i t^{1/2} + C \quad (6)$$

where C is the intercept and k_i is the intraparticle diffusion rate constant ($mg/g\,min^{1/2}$) which can be evaluated from the slope of the linear plot of q_t vs. $t^{1/2}$. The pseudo-first and -second order rates and intraparticle diffusion rate equations, values of constants and correlation coefficient for fluoride removal by PAN-oxime-nano Fe_2O_3 are shown in Table 2.

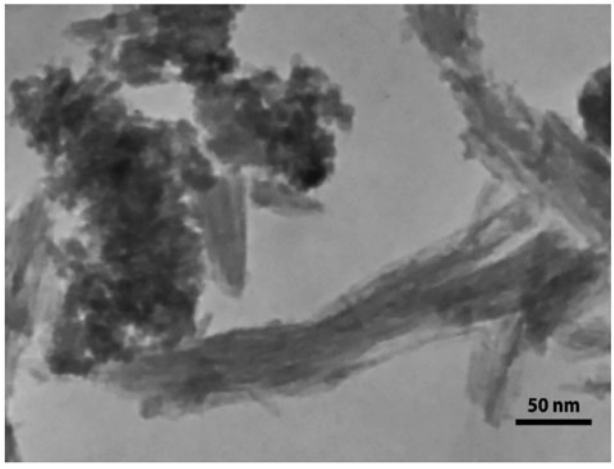

Fig. 3. TEM image of functionalized-PAN–Fe_2O_3.

Table 1
Constant of Freundlich and Langmuir isotherm of fluoride

Langmuir model: $\frac{1}{q_e} = \frac{1.359}{c_e} + 0.004$

q_m(mg/g)	b (l/mg)	R^2
250	0.0029	0.989

Freundlich model: $\ln q_e = 0.89\ \ln C_e - 0.066$

k_f (mg/g)	N	R^2
0.557	1.123	0.956

Table 2
Pseudo-first and second-order and intraparticle diffusion model parameters

Pseudo-first-order rate: $\ln(q_e - q_t) = -0.028t + 3.579$		
q_e (mg/g)	k_1 (l/min)	R^2
19.707	0.028	0.995
Pseudo-second-order rate: $t/q_t = 47.33t - 31.38$		
q_e (mg/g)	k_2 (g/mg min)	R^2
0.021	71.42	0.955
Intraparticle diffusion rate: $q_t = 3.037t^{1/2} + 4.98$		
k_i (mg/g min $^{1/2}$)	C (mg/g)	R^2
3.037	4.98	0.955

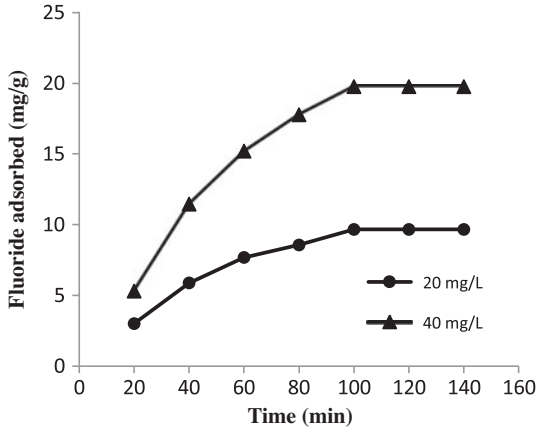

Fig. 4. Effect of contact time on fluoride adsorption rate for different initial fluoride concentrations.

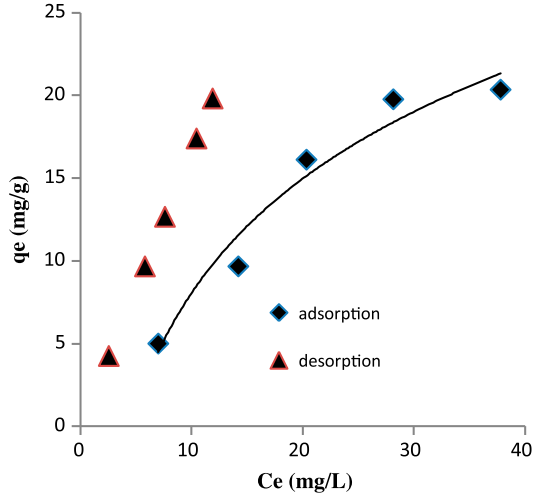

Fig. 5. Adsorption and desorption isotherms of fluoride on the PAN-oxime-nano Fe_2O_3.

3.3. Desorption

The experimental data of adsorption–desorption of fluoride on the PAN-oxime-nano Fe_2O_3 as well as the adsorption isotherm are shown in Fig. 5. If the adsorption equilibrium data were on the adsorption isotherm, the adsorption would be reversible.

4. Discussion

4.1. Adsorption experiment

Adsorption isotherm is a dynamic concept reached when the rate at which molecules adsorb on to the surface is equal to the rate at which they desorb. The equilibrium adsorption isotherm's shape is of great importance to provide information about the adsorbents' surface structure. The data obtained indicated that adsorption of fluoride onto PAN-oxime-nano Fe_2O_3 was better explained by Langmuir isotherm with $R^2 = 0.989$ (Table 1), which evidence that there is no interaction between the adsorbate molecules and that the adsorption occurs in monolayer. Another important parameter, R_L, the separation factor or equilibrium parameter is determined from the relation:

$$R_L = \frac{1}{1 + bC_0} \tag{7}$$

where b is the Langmuir constant and C_0 (mg/L) is the initial fluoride concentration. The value of R_L shows the type of isotherm to be either favorable ($0 < R_L < 1$), unfavorable ($R_L > 1$), linear ($R_L = 1$), or irreversible ($R_L = 0$). The R_L value in the present study is 0.87, which confirms that adsorption of fluoride with this material is favorable under the conditions of this research. k and n are Frundlich constants, n gives an indication of how favorable the adsorption process is. It is generally known that values of n in the range of 2–10 shows good, 1–2 approximately difficult, and less than 1 poor adsorption property. PAN-oxime-nano Fe_2O_3 stated moderately difficult behavior ($1 < n < 2$) in this experiment. The slope $1/n$ ranging between 0 and 1 is a measure of adsorption intensity or surface heterogeneity. As this value reached to 0, the surface becomes more heterogeneous. In this experiment, $1/n$ equals 0.89 which shows that the surface is not heterogeneous.

4.2. Kinetic analysis

The effect of contact time and initial fluoride concentration on the removal of Fluoride by PAN-oxime-nano Fe_2O_3 is shown in Fig. 4. A rather fast uptake occurs during the first 60 min of adsorption process followed by a slower stage as the adsorbed amount of

flouride reaches its equilibrium value. It is also demonstrated that as the initial fluoride concentration increased, the adsorption capacity increased.

The R^2 values of the pseudo-first-order and second-order models exceeded 0.95 (Table 2) but due to the higher R^2 values obtained from pseudo-first order model, this model represented better adsorption kinetics. Typically, various mechanisms control the adsorption kinetics, the most limiting is the diffusion which includes external diffusion, boundary layer diffusion, and intraparticle diffusion [25]. When the line of intraparticle diffusion model passes through the origin (C=0), the intraparticle diffusion will be the sole rate-control step. The regression in our study did not pass through the origin (Table 2) suggesting that the adsorption of fluoride onto PAN-oxime-nano Fe_2O_3 involved intraparticle diffusion, but that was not the only rate-controlling step.

4.3. Reversibility of fluoride adsorption on PAN-oxime-nano Fe_2O_3

The reversibility of fluoride adsorption was studied by carrying out adsorption–desorption experiments. If the desorption equilibrium data was on the adsorption isotherm curve, the adsorption would be irreversible. Hysteresis and irreversibility have also been interchangeably used in the literature [26]. It can be observed in Fig. 5 that the desorption equilibrium data was above the adsorption isotherm. Adsorption–desorption hysteresis present irreversible for fluoride suggesting that the fluoride adsorption onto PAN-oxime-nano Fe_2O_3 was not reversible. Desorption of pollutants from adsorbents is of critical importance to most environmental concerns because this process affects chemical fate, toxicity, and associated risks to human and aquatic life as well as the feasibility and the necessity of remediation technologies [27]. If the pollutants would not be released from the adsorbent in significant concentrations, either in the environmental or biotic mediums, they would be safe to living organisms. In this work, the quantity of fluoride retained by PAN-oxime-nano Fe_2O_3 was lower, based on the sorption isotherm, compared with the corresponding desorption isotherm suggesting that adsorption/desorption of fluoride on PAN-oxime-nano Fe_2O_3 is hysteretic and reactions involved in the sorption process may be irreversible or very slowly reversible.

5. Conclusion

The results from the present study show the potential of PAN-oxime-nano Fe_2O_3 for fluoride removal. The adsorption capacity increased with increasing initial fluoride concentration. The equilibrium data were analyzed using the Langmuir and Freundlich isotherm models. The equilibrium data fit very well with the Langmuir isotherm equation. The adsorption data were modeled using pseudo-first and second-order kinetic equations and intraparticle diffusion models. The Pseudo-first-order kinetic equation best described the sorption kinetics.

Acknowledgment

This research was supported by Medical Science Research Center, Tehran Medical Branch, Islamic Azad University, Tehran, Iran and technical laboratory support of KimiaFaam pharmaceutical Company.

References

[1] World Health Organization, Guidelines for Drinking-Water Quality: Incorporating First Addendum Recommendations, vol. 1, third ed., World Health Organization, 20 Avenue Appia, 121 Geneva 27, Switzerland, 2006, pp. 375–376.
[2] D. Ortiz-Péreza, M. Rodríguez-Martínezb, F. Martínezb, V.H. Borja-Aburtoc, J. Castelod, J.I. Grimaldoe, D. Cruze, L. Carrizales, F. Díaz-Barriga, Fluoride induced disruption of reproductive hormones in men, Environ. Res. 93 (2003) 20–30.
[3] WHO Report, Fluoride and Fluorides: Environmental Health Criteria, World Health Organisation, 1984.
[4] Alain Tressaud (Ed.), Advances in Fluorine Science, Fluorine and the Environment, Agrochemicals, Archaeology, Green Chemistry & Water, vol. 2, Elsevier, 2006.
[5] S. Ghorai, K.K. Pant, Equilibrium, kinetics, and breakthrough studies for adsorption of fluoride on activated alumina, Sep. Purif. Technol. 42 (2005) 265–271.
[6] C.J. Huang, J.C. Liu, Precipitate flotation of fluoride-containing wastewater from a semiconductor manufacturer, Water Res. 33 (1999) 3403–3412.
[7] M.G. Sujana, R.S. Thakur, S.B. Rao, Removal of fluoride from aqueous solution by using alum sludge, J. Colloid Interf. Sci. 206 (1998) 94–101.
[8] C. Castel, M. Schweizer, M.O. Simonnot, M. Sardin, Selective removal of fluoride ions by a two-way ion-exchange cyclic process, Chem. Eng. Sci. 55 (2000) 3341–3352.
[9] Z. Amor, B. Bernard, N. Mameri, M. Taky, S. Nicolas, A. Elmidaoui, Fluoride removal corn brackish water by electrodialysis, Desalination 133 (2001) 215–223.
[10] N. Bensalah, B. Louhichi, A. Abdel-Wahab, Electrochemical oxidation of succinic acid in aqueous solutions using boron doped diamond anodes, Int. J. Environ. Tech. 9 (2012) 135–143.
[11] M. Mohapatra, S. Anand, B.K. Mishra, D.E. Giles, P. Singh, Review of fluoride removal from drinking water, J. Environ. Manage. 91 (2009) 67–77.
[12] H. Sepehrian, M. Samadfam, Z. Asadi, Studies on the recovery of uranium from nuclear industrial effluent using nanoporous silica adsorbent, Int. J. Environ. Sci. Tech. 9 (2012) 629–636.
[13] F. Mastali Khan Tehrani, M. Rashidzadeh, M. Nemati, A. Irandoukht, B. Faridnia, Characterization and photocatalytic activities of nanosized titanium dioxide thin films, Int. J. Environ. Sci. Tech. 8 (2011) 545–552.

[14] E. Kumar, A. Bhatnagar, U. Kumar, M. Sillanpää, Defluoridation from aqueous solutions by nano-alumina: Characterization and sorption studies, J. Hazard. Mater. 186 (2011) 1042–1049.
[15] C. Viswanathan, N. Sairam Sundaram, S. Meenakshi, Uptake of fluoride by nano hydroxyapatite/chitosan, a bioinorganic composite, Bioresource Technol. 99 (2008) 8226–8230.
[16] Xi. Zhaoa, J. Wanga, F. Wub, T. Wanga, Y. Caia, Y. Shia, G. Jianga, Removal of fluoride from aqueous media by Fe_3O_4@$Al(OH)_3$ magnetic nanoparticles, J. Hazard. Mater. 173 (2010) 102–109.
[17] K.E. Perepelkin, N.V. Klyuchnikova, N.A. Kulikova, Experimental evaluation of man-made fibre brittleness, Fibre Chem. 21 (1989) 145–148.
[18] M.S.A. Rahaman, A.F. Ismail, A. Mustafa, A review of heat treatment on polyacrylonitrile fiber, Polym. Degrad. Stab. 92 (2007) 1421–1432.
[19] Y.J. Bai, C.G. Wang, N. Lun, Y.X. Wang, M.J. Yu, B. Zhu, HRTEM microstructures of PAN precursor fibers, Carbon 44 (2006) 1773–1778.
[20] X. Chang, Q. Su, D. Liang, X. Wei, B. Wang, Efficiency and application of poly (acryldinitrophenylamidrazone–dinitroacrylphenylhydrazine) chelating fiber for pre-concentrating and separating trace Au(III), Ru(III), In(III), Bi(III), Zr(IV), V(V), Ga(III) and Ti(IV) from solution samples, Talanta 16 (2002) 253–261.
[21] S. Khalid, H. Sajjad, T.J. Oh, P. Soo-Young, Preparation of amidoxime-modified polyacrylonitrile (PAN-oxime) nanofibers and their applications to metal ions adsorption, J. Membr. Sci. 322 (2008) 400–405.
[22] F. Yang, W. Zheng, H. Huang, Z. Li, H.N. Zhang, W. Wang, C. Wang, Decoration of electrospun nanofibers with magnetic nanoparticles via electrospinning and sol–gel process, Chem. Res. 26 (2010) 847–850.
[23] Y.S. Ho, G. McKay, Pseudo-second-order model for sorption processes, Process Biochem. 34 (1994) 451–465.
[24] W.J. Weber, J.C. Morris, Kinetics of adsorption on carbon from solution, J. Sanit. Eng. Div. 89 (1963) 31–59.
[25] D. Wankasi, M. Horsfall, A.I. Spiff, Retention of Pb(II) ion from aqueous solution by nipah palm (nypa fruticans wurmb) petiole biomass, J. Chil. Chem. Soc. 50 (2005) 691–696.
[26] N. Zamani, Hexamine adsorption study on activated carbon from aqueous solutions for application in treatment of hexamine industrial wastewater, Int. J. Environ. Sci.Tech. 10 (2013) 19–26.
[27] E. Guibal, P. McCarrick, J.M. Tobin, Comparison of the adsorption of anionic dyes on activated carbon and chitosan derivatives from dilute solutions, Sep. Sci. Technol. 38 (2003) 3049–3073.